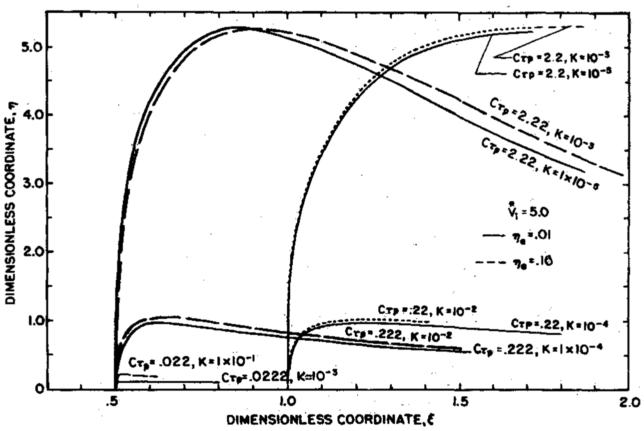

Fig. 1 Particle trajectories for the case of $\overset{*}{V}_i = 5.0$.

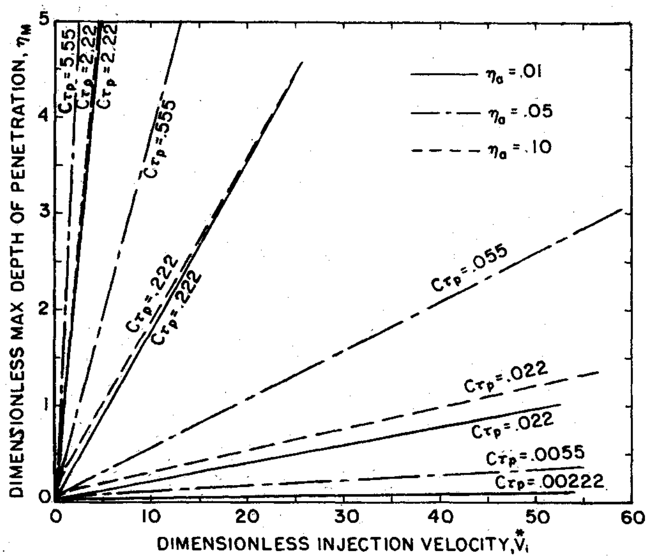

Fig. 2 Maximum penetration depth as a function of injection velocity.

for $c\tau_p > 0.10$, η_m is, for all practical purposes, independent of η_a and for a given $c\tau_p$ is determined only by $\overset{*}{V}_i$. Recall that for Hiemenz flow, the edge of the boundary layer corresponds to $\eta \simeq 2.4$. Consequently, Fig. 2 automatically yields, for a given $c\tau_p$, the dimensionless injection velocity required to reach the edge of the boundary layer.

References

[1] Petscheck, H., Adamis, D., and Kantrowitz, A. R., "Stagnation Flow Thrombus Formation," *Transactions of the American Society of Artificial Internal Organs*, Vol. 14, 1968, pp. 256–259.

[2] Fuchs, N. A., *Mechanics of Aerosols*, Pergamon Press, London, 1964.

[3] Otterman, B and Yau, F., "Motion of Small Particles within the Stagnation of Region of a Viscous-Incompressible Fluid," *Proceedings of the Society of Engineering Science*, 8th Annual Meeting, Washington, D.C., 1970.

[4] Saffman, P. G., "The Lift on a Small Sphere in a Slow Shear Flow," *Journal of Fluid Mechanics*, Vol. 22, Pt. 2, 1965, pp. 385–400.

[5] Saffman, P. G., "Corrigendum," *Journal of Fluid Mechanics*, Vol. 31, Pt. 3, 1968, p. 624.

[6] Rubinow, S. I. and Keller, J. B., "The Transverse Force on a Spinning Sphere Moving in a Viscous Fluid," *Journal of Fluid Mechanics*, Vol. 11, 1961, pp. 447–459.

[7] Brenner, H., *Advances in Chemical Engineering*, Vol. 6, Academic Press, New York, 1966.

[8] Lawler, M. T. and Lu, P. C., "A Study of Radial Migrations in Fluid-Particle Flows with Fluid Rotation," *Advances in Solid-Liquid Flows in Pipes and Its Application*, edited by I. Zandi, Pergamon Press, New York, 1971.

[9] Fuchs, N. A., *Mechanics of Aerosols*, Pergamon Press, London, 1964, p. 75.

[10] Schlichting. H., *Boundary Layer Theory*, McGraw-Hill, New York, 1955.

[11] Yau, F. F. P., "Motion of Particles in Laminar Flows of Solid-Fluid Mixtures," M.S. thesis, 1970, Dept. of Mech. Engineering, Northeastern Univ., Boston, Mass.

Hypersonic Viscous, Slip Flow over Insulated Wedges

AJAY KUMAR* AND A. C. JAIN†

Indian Institute of Technology, Kanpur, India

Nomenclature

c	$= \mu_w T_\infty / \mu_\infty T_w$, Chapman-Rubesin constant
c_f	$= \tau / \frac{1}{2}\rho_\infty u_\infty^2$
C_p	= specific heat at constant pressure
H	= total enthalpy
k	= thermal conductivity
M	= Mach number
p, ρ, T	= pressure, density, and temperature, respectively
Pr	= Prandtl number
R	= gas constant
Re_x	$= u_\infty \rho_\infty x / \mu_\infty$
u, v	= velocity components along x, y directions
u_b	= slip velocity
x, y	= distances along and perpendicular to the wedge surface
ξ, η	= defined in Eq. (12)
β	= semiwedge angle
γ	= ratio of specific heats
δ	= boundary-layer thickness
θ_s	$= \beta + d\delta/dx$, local slope of the boundary-layer edge with free-stream
λ	= mean free path
τ	$= \mu_w (\partial u/\partial y)_w$
μ	= coefficient of viscosity
$\bar{\chi}$	$= M_\infty^3 (c/Re_x)^{1/2}$, strong interaction parameter

Subscripts

∞	= conditions in freestream
e	= conditions at the edge of the boundary layer
w	= conditions at the wall

Introduction

SHEN[1] investigated the hypersonic flow past an insulated wedge with no slip boundary conditions at the surface. He found that boundary-layer thickness varies as $(x)^{3/4}$ and pressure ratio (p_w/p_∞) varies as $(x)^{-1/2}$. This indicates that pressure ratio tends to infinity as leading edge is approached. Aroesty[2] investigated the slip effects in the strong interaction region by taking slip velocity as a perturbation to the no slip case. Here, we modified Shen's solution over the wedge by incorporating the effect of slip velocity at the surface. An inviscid flow is envisaged in between the shock wave and the boundary layer. Tangent-wedge approximation provides the pressure distribution at the

Received August 4, 1971; revision received March 2, 1972. This work was supported by the Ministry of Defence, Government of India, under a Grant-in-Aid Project entitled "Hypersonic Flow at Low Reynolds Numer."

Index category: Supersonic and Hypersonic Flow.

* Senior Research Fellow, Department of Aeronautical Engineering.

† Assistant Professor, Department of Aeronautical Engineering.

edge of the boundary layer. Kârmân-Pohlhausen method is used with linear profile for tangential component of velocity in the boundary layer. An analytical solution is obtained in the leading edge region. Governing equations are, then, integrated numerically for various semiwedge angles. The numerical solution agrees with the analytical solution in the leading edge region and provides solution further downstream.

Equations of Motion and Their Solution

Governing equations of a 2-dimensional steady flow on a wedge are the following:

$$(\partial/\partial x)(\rho u)+(\partial/\partial y)(\rho v)=0 \quad (1)$$

$$\rho u\,\partial u/\partial x+\rho v\,\partial u/\partial y=-(dp/dx)+(\partial/\partial y)(\mu\,\partial u/\partial y) \quad (2)$$

$$\rho u\,\partial H/\partial x+\rho v\,\partial H/\partial y=(\partial/\partial y)[(\mu/Pr)\partial H/\partial y+(1-1/Pr)\mu(\partial/\partial y)(\tfrac{1}{2}u^2)] \quad (3)$$

$$p=R\rho T \quad (4)$$

Boundary conditions are

at $\quad y=0,\quad v=0,\quad u=u_b=C_1\lambda_w(\partial u/\partial y)_w \quad$ (5a)

where

$$C_1\simeq(\pi/2)^{1/2}\quad\text{and}\quad \lambda_w=1.256\gamma^{1/2}\mu_w/a_w\rho_w$$

at $\quad y=\delta,\quad u=u_e\simeq u_\infty,\quad T=T_e \quad$ (5b)

For $Pr=1$ and in the presence of slip velocity with adiabetic wall, there exists the following integral of the energy equations, Eq. (3):

$$H=H_e=H_\infty$$

Neglecting terms of second order in λ_w, we get the adiabetic wall temperature as

$$T_w/T_\infty=1+[(\gamma-1)/2]M_\infty^{\ 2}\simeq[(\gamma-1)/2]M_\infty^{\ 2} \quad (6)$$

From Eqs. (1) and (2), in the presence of slip velocity on the surface, we get the following Kârmân's integral:

$$\frac{d}{dx}\int_0^\delta \rho u(u_\infty-u)\,dy=(dp/dx)\delta+\mu_w(\partial u/\partial y)_w \quad (7)$$

Assuming

$$u/u_\infty=A+By \quad (8)$$

and using boundary condition (5a) and (5b), we get,

$$u/u_\infty=(C_1\lambda_w+y)/(C_1\lambda_w+\delta) \quad (9)$$

Substituting (9) in (7) and neglecting terms of second order of smallness [e.g., $C_1^{\ 2}\lambda_w^{\ 2}/\delta^2$, $(\lambda_w/\delta)\,d\delta/dx$ etc.], we get

$$\delta\,dp/dx+2p\,d\delta/dx=\mu_w u_\infty/(C_1\lambda_w+\delta) \quad (10)$$

From tangent-wedge approximation

$$p/p_\infty=[\gamma(\gamma+1)/2]M_\infty^{\ 2}\theta_s^{\ 2}=[\gamma(\gamma+1)/2]M_\infty^{\ 2}(\beta+d\delta/dx)^2 \quad (11)$$

Nondimensionalizing the variables in Eq. (10) as follows:

$$\eta=\delta/L,\ \xi=x/L\quad \text{where}\,L=\mu_w/u_\infty\rho_\infty \quad (12)$$

and substituting Eq. (11) in Eq. (7), we get

$$\eta\eta'\eta''+\eta'^3+\beta(\eta\eta''+\beta\eta'+2\eta'^2)=[1/(\gamma+1)]\,1/(\eta+C_1\lambda_w/L) \quad (13)$$

where prime denotes differentiation with respect to ξ. Here

$$(C_1\lambda_w/L)(\beta+\eta')^2=e \quad (14)$$

where

$$e=[1.256/(\gamma+1)]C_1[2(\gamma-1)/\gamma]^{1/2}$$

Using Eq. (14) in Eq. (13), we get

$$e[\eta'(\eta'+\beta)+\eta\eta'']+\eta\eta'(\eta'+\beta)^3+\eta^2\eta''(\eta'+\beta)^2=(b/2)(\eta'+\beta) \quad (15)$$

where

$$b=2/(\gamma+1)$$

Let

$$\eta=\xi^\sigma\sum^{\infty}a_n\xi^{nq} \quad (16)$$

Substituting Eq. (16) in Eq. (15) and collecting terms of like powers of ξ, we find that for slip to be a dominant phenomenon near the leading edge

$$\sigma=1\quad\text{and}\quad q=1$$

Hence

$$\eta=\xi(a_0+a_1\xi+a_2\xi^2+\ldots) \quad (17)$$

where

$$a_0=b/2e,\quad a_1=-b^2(b+2e\beta)^3/64e^5(b+e\beta)$$

$$a_2=-\frac{2}{3}\left[\frac{6ea_1^{\ 2}+3a_0a_1\beta^3+17a_0^{\ 2}a_1\beta^2+25a_0^{\ 3}a_1\beta+11a_0^{\ 4}a_1}{3b+2e\beta}\right]$$

We also integrated Eq. (15) numerically for various semiwedge angles. The numerical solution agrees with the analytical solution in the leading edge region and provides solution further downstream.

Discussion and Results

In Fig. 1, slip velocity is plotted against $M_\infty(c/Re_x)^{1/2}$ for various semiwedge angles. It shows that slip velocity decreases with increase in semiwedge angle. At the leading edge, it tends to a constant value which is nearly 90% of the freestream velocity. Further, slip velocity is not zero even in the strong interaction region. Figure 2 shows that slip reduces boundary-layer thickness δ but the reduction in δ is smaller as β becomes larger.

Figure 3 shows that in the presence of slip, pressure tends to a constant value as leading edge is approached while it tends to infinity in the absence of slip. It is seen that slip reduces the pressure level and the pressure increases as the semi-wedge angle

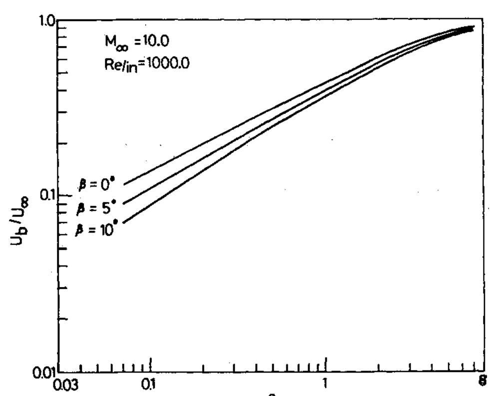

Fig. 1 Variation of slip velocity with $\bar{\chi}/M_\infty^{\ 2}$.

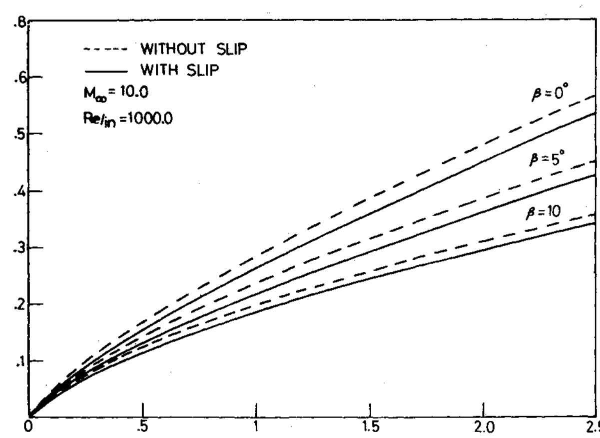

Fig. 2 Viscous layer edge vs the distance along the wedge.

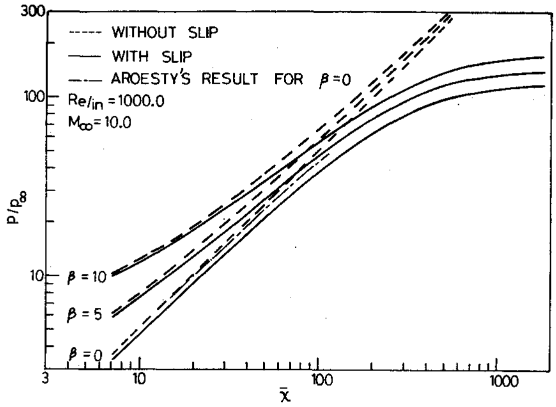

Fig. 3 Variation of p/p_∞ with $\bar{\chi}$.

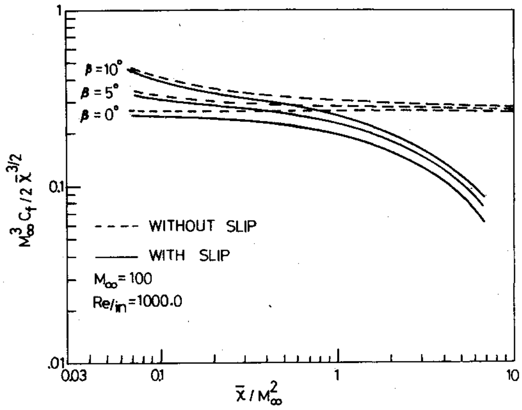

Fig. 4 Variation of $M_\infty{}^3 c_f/2\bar{\chi}^{3/2}$ with $\bar{\chi}/M_\infty{}^2$.

is increased. As expected, due to slip, Aroesty's result shows a slight decrease in pressure from the strong interaction value.

In Fig. 4, skin-friction coefficient is plotted against the rarefaction parameter $M_\infty (c/Re_x)^{1/2}$. It is seen again that slip reduces the skin friction. Also, increase in semiwedge angle increases skin friction. Sufficiently far downstream, both pressure and skin friction tend to their strong interaction value, respectively.

References

[1] Shen, S. F., "An Estimate of Viscosity Effects on the Hypersonic Flow over an Insulated Wedge," *Journal of Mathematics and Physics*, Vol. 31, 1952, pp. 192–205.

[2] Aroesty, J., "Slip Flow and Hypersonic Boundary Layers," *AIAA Journal*, Vol. 2, No. 1, Jan. 1964, pp. 189–190.

Statics of Transversely Isotropic Beams

E. J. Brunelle*

Rensselaer Polytechnic Institute, Troy, N. Y.

Introduction

Recent papers[1–4] have demonstrated a few instances in which transverse isotropy plays a significant role in beam or plate analysis. These studies are potentially important since many of the newer materials considered for use in aerospace structural applications exhibit transverse isotropy. However, it is not generally realized that transverse isotropy plays a significant role in all kinds of static and dynamic analyses. Thus it is the purpose of this Note to provide a brief study of the effects of transverse isotropy on a variety of static beam problems.† The problems considered are the determination of Green's functions (influence functions), static deflections due to distributed loads, and beam-column deflections.‡ It will be shown that the effects of transverse isotropy can be quite dramatic, particularly when the beam boundary restraints are increased.

Received August 18, 1971; revision received April 20, 1972.

Index category: Structural Static Analysis.

* Associate Professor of Aeronautics and Astronautics, Department of Aeronautics and Astronautics. Member AIAA.

Static Equations of Motion

Assuming displacements of the form $u(x, z) = z\psi(x)$ and $w(x, z) = w_0(x) + w(x)$, the needed strain-displacement relations are given by

$$\varepsilon_x = z d\psi/dx, \quad \varepsilon_{xz} = \tfrac{1}{2}(\psi + dw/dx) \tag{1}$$

Defining the in-plane modulus of elasticity to be E, the transverse shear modulus to be G^*, and Mindlin's shear correction factor to be κ^2 (which we will assume to be $\pi^2/12$), the stress-strain laws are given by

$$\sigma_x = Ez d\psi/dx, \quad \sigma_{xz} = \kappa^2 G^*(\psi + dw/dx) \tag{2}$$

Using (2), the shear and moment resultants are given by

$$Q_x = \kappa^2 G^* A^*(\psi + dw/dx) \tag{3}$$

$$M_x = -EI\, d\psi/dx \tag{4}$$

where $A^* = bh$, $I = bh^3/12$, b is the beam width and h is the beam depth. The sum of the vertical forces and y axis moments are given by

$$q + dQ_x/dx + N_x d^2(w + w_0)/dx^2 = 0 \tag{5}$$

$$dM_x/dx + Q_x = 0 \tag{6}$$

where q = transverse distributed loading; w_0 = initial (unstressed) displacement; N_x = in-plane load. Putting (3) and (4) into (5) and (6) yields coupled equations for w and ψ. That is,

$$\kappa^2 G^* A^*(d\psi/dx + d^2w/dx^2) + N_x d^2w/dx^2 = -N_x d^2w_0/dx^2 - q \tag{7}$$

$$-EI\, d^2\psi/dx^2 + \kappa^2 G^* A^*(\psi + dw/dx) = 0 \tag{8}$$

Green's Functions

Rearranged forms of (3) and (4), that is

$$d\psi/dx = -M_x/EI \tag{9}$$

$$dw/dx = (Q_x/\kappa^2 G^* A^*) - \psi \tag{10}$$

are used to determine Green's functions for statically determinate beams in the following fashion: for a given M_x and Q_x (in the regions $0 \leqq x \leqq \zeta$ and $\zeta \leqq x \leqq l$), due to a specified unit generalized load (either force or moment), (9) may be integrated to find ψ and then this result entered into (10) determines w after another integration. The constants of integration are determined by the boundary conditions and by the matching conditions (slope and displacement) at the interface $x = \xi$.

For a cantilever beam we find that the complete set of Green's functions is given by,

$$\begin{aligned}
\overset{\delta F}{C}(x,\xi) &= \begin{cases} (x/6EI)[x(3\xi - x) + 6l^2 S^*]\,; & x \leqq \xi \\ (\xi/6EI)[\xi(3x - \xi) + 6l^2 S^*]\,; & x \geqq \xi \end{cases} \\
\overset{\delta M}{C}(x,\xi) &= \begin{cases} (x^2/2EI) & ; x \leqq \xi \\ (\xi/2EI)(2x - \xi) & ; x \geqq \xi \end{cases} \\
\overset{\psi F}{C}(x,\xi) &= \begin{cases} (x/2EI)(x - 2\xi) & ; x \leqq \xi \\ (-\xi^2/2EI) & ; x \geqq \xi \end{cases} \\
\overset{\psi M}{C}(x,\xi) &= \begin{cases} (-x/EI) & ; x \leqq \xi \\ (-\xi/EI) & ; x \geqq \xi \end{cases}
\end{aligned} \tag{11}$$

† Dynamic problems will be considered in a sequel Note.

‡ Buckling problems have been treated previously[2,3] and thus will not be treated in this Note.